THE ASTRONOMICAL JOURNAL, 120:1946–1953, 2000 October

THE COLD AND HOT GAS CONTENT OF FINE-STRUCTURE E AND S0 GALAXIES

A. E. SANSOM
Centre for Astrophysics, University of Central Lancashire, Preston PR1 2HE, UK; a.e.sansom@uclan.ac.uk
J. E. HIBBARD
National Radio Astronomy Observatory,[1] 520 Edgemont Road, Charlottesville, VA 22903; jhibbard@nrao.edu
AND
FRANÇOIS SCHWEIZER
Observatories of the Carnegie Institution of Washington, 813 Santa Barbara Street, Pasadena, CA 91101-1292; schweizer@ociw.edu
Received 2000 May 15; accepted 2000 June 27

ABSTRACT

We investigate trends of the cold and hot gas content of early-type galaxies with the presence of optical morphological peculiarities, as measured by the fine-structure index Σ. H I mapping observations from the literature are used to track the cold gas content, and archival *ROSAT* Position Sensitive Proportional Counter data are used to quantify the hot gas content. We find that E and S0 galaxies with a high incidence of optical peculiarities are exclusively X-ray underluminous and, therefore, deficient in hot gas. In contrast, more relaxed galaxies with little or no signs of optical peculiarities span a wide range of X-ray luminosities. That is, the X-ray excess anticorrelates with Σ. There appears to be no similar trend of cold gas content with either fine-structure index or X-ray content. The fact that only apparently relaxed E and S0 galaxies are strong X-ray emitters is consistent with the hypothesis that after strong disturbances, such as a merger, hot gas halos build up over a timescale of several gigayears. This is consistent with the expected mass loss from stars.

Key words: galaxies: evolution — galaxies: ISM — galaxies: peculiar

1. INTRODUCTION

In the merger hypothesis for elliptical galaxy formation (Toomre & Toomre 1972), spiral galaxies coalesce to produce elliptical galaxies. If this is a common mechanism for the formation of elliptical galaxies, then it requires that the cold gas present in the spiral progenitors (typically $\sim 10^9$–10^{10} $M_\odot$) be lost or heated, since similar quantities of cold gas are not generally detected in elliptical galaxies (Knapp, Turner, & Cunniffe 1985a; Lees et al. 1991; Roberts et al. 1991). On the other hand, elliptical and S0 (i.e., early-type) galaxies are found to be much more X-ray luminous than spirals at a given blue luminosity, L_B. While there is scatter of 2 orders of magnitude in the relationship between the X-ray luminosity L_X and L_B, early-type galaxies follow a much steeper relationship than spirals (Fabbiano, Kim, & Trinchieri 1992; Beuing et al. 1999). It is, therefore, of interest to examine the state of the interstellar medium (ISM) in merger remnants to see whether cold gas is being converted into other phases. Early-type galaxies showing morphological or kinematic peculiarities are suggested to be these postmerger objects (Schweizer 1986; Schweizer et al. 1990; Bender & Surma 1992; Schweizer & Seitzer 1992, hereafter SS92).

Ideally, one would like to trace the evolution of the cold, warm, and hot gas phases along a sequence of progressively more evolved merger remnants. This requires an observational characteristic that tracks the time elapsed since merging. To this end, Schweizer et al. (1990) introduced a fine-structure index Σ to quantify the presence of ripples, jets of luminous matter, the boxiness of isophotes, etc. Elliptical galaxies and S0 galaxies with larger values of Σ were statistically shown to have observational characteristics (colors and spectral line strengths) consistent with the presence of younger stellar populations, supporting the idea that they represent more recent mergers in which starbursts have occurred (Schweizer et al. 1990; SS92). These galaxies were suggested to be ∼2–10 Gyr old relics of ancient mergers populating the so-called King gap between ∼1 Gyr old remnants and old elliptical galaxies (I. King, quoted in Toomre 1977).

The X-ray properties of a sequence of *ongoing* mergers was studied by Read & Ponman (1998). They found that, following early increases in the emission from hot gas, examples of relaxed remnants at ∼1.5 Gyr after a merger appear relatively devoid of such gas (see also Hibbard et al. 1994). For normal galaxies of early Hubble type, Bregman, Hogg, & Roberts (1992) noted a striking lack of correlations between the hot and cold interstellar gas components. Toward later Hubble types, they found a general increase of the cold-to-hot gas ratio and interpreted this systematic change as evidence that cold gas is a phenomenon associated with disks, while hot gas is associated with bulge components.

In this paper we examine the cold and hot atomic gas contents of early-type galaxies studied by SS92, which have also been mapped in the 21 cm line of neutral hydrogen (H I) or observed in X-rays with *ROSAT* and its PSPC detector. By looking for trends with Σ, we hope to trace the fate of gas as merger remnants evolve. Preliminary work in this area was carried out by Fabbiano & Schweizer (1995) and Mackie & Fabbiano (1997), who showed that three dynamically young elliptical galaxies with fine structure (NGC 3610, 4125, and 4382) were low X-ray emitters. We build upon this earlier work by expanding the number of galaxies with both fine structure and X-ray content quantified and by including information on the cold atomic gas content as well. Section 2 describes the SS92 sample of

[1] The National Radio Astronomy Observatory is a facility of the National Science Foundation operated under cooperative agreement by Associated Universities, Inc.

galaxies, while § 3 presents a compilation of archival *ROSAT* observations for galaxies from that sample. In § 4, we examine separately and then together the presence of H I and X-ray emission in the SS92 sample to understand whether galaxies with fine structure are King gap objects, and, if so, what we can learn about the fate of cold gas in disk-disk mergers and the origin of X-ray halos in elliptical galaxies. Finally, § 5 summarizes our conclusions.

2. SAMPLE DESCRIPTION

To look at correlations between cold and hot gas content and fine structure, we took the sample of SS92. This sample consists of 69 E and S0 galaxies plus the two merger remnants NGC 3921 and NGC 7252. With the exception of the latter two objects, all sample galaxies lie north of $\delta = -20°$ and at $|b| > 20°$, have apparent magnitudes $B_T \leq 13.5$, and have recession velocities $v_0 < 4000$ km s^{-1}. The two merger remnants have $v_0 < 6000$ km s^{-1}. Five of the sample galaxies are members of the Virgo Cluster, while all the others are either field objects or in loose groups. The absolute magnitudes range between $M_B = -18.4$ and -21.6, with a median value of -20.3 (for $H_0 = 75$ km s^{-1} Mpc^{-1}). The merger remnants NGC 3921 and NGC 7252 were included because of their extremely rich fine structure and evolutionary status as likely proto–elliptical galaxies (Toomre & Toomre 1972; Barnes 1994; Hibbard et al. 1994; Schweizer 1996).

The fine structure of these galaxies was studied by SS92 on CCD images obtained in the *R* passband with the KPNO 0.9 m telescope. For each galaxy, a fine-structure index Σ was derived. This index is defined as $\Sigma = S + \log(1 + n) + J + B + X$, where S is a visual estimate of the strength of the most prominent ripples ($S =$ 0–3), n is the number of detected ripples ($n =$ 0–17), J is the number of luminous plumes or "jets" ($J =$ 0–4), B is a visual estimate of the maximum boxiness of isophotes ($B =$ 0–3), and X indicates the absence or presence of an X structure ($X = 0$ or 1). The values of Σ for the present sample of galaxies cover the range 0–10.1. The correlation of Σ with optical colors and line strengths supports its use as an indicator of ancient mergers (SS92). High-Σ systems are unlikely to have formed from minor perturbations or internal instabilities, particularly those with tidal tails or jets indicative of kinematically cold progenitors. By design, Σ measures four types of fine structure thought to be caused by mergers and can serve as a rough measure of dynamical youth or rejuvenation (for detailed review, see Schweizer 1998).

3. *ROSAT* DATA

For the hot gas content, we first cross-correlated the SS92 list against the *ROSAT* Position Sensitive Proportional Counter (PSPC) archive (within 20′ of the PSPC field centers), which yielded pointed X-ray observations for 28 of the 71 sample galaxies. X-ray fluxes were obtained from PSPC images using the broadband (0.1–2.4 keV) images from the *ROSAT* PSPC archive at Leicester University. We visually inspected the images to select source and background regions. We then used a circular aperture of between 1′ and 7′ radius R (depending on source extent) to estimate source counts. Background counts in the source detection cell were estimated using either an annulus or offset area, depending on where other sources lay in the field. To estimate fluxes from these source counts, we had to adopt an integrated H I column density ($N_{H\,I}$) due to our Galaxy. Such column densities were obtained from the data of Stark et al. (1992) using a program written by K. Arnaud. We assumed a thermal source spectrum of solar metallicity and $kT = 0.5$ keV (typical of many ellipticals; Brown & Bregman 1998). Using the *ROSAT* announcement-of-opportunity document, we could then estimate conversion factors to convert our source counts to fluxes (to within 10%–20%, allowing for a temperature range of 0.3 keV $< kT <$ 1.0 keV). One-sigma errors on fluxes are a combination of Poisson errors on source counts, including background uncertainty and estimated errors on the conversion factor. These results are presented in Table 1. The galaxies NGC 596 and NGC 4283 were undetected, whence 3 σ upper limits are given for the source counts and fluxes in these two cases.

To try to increase the sample size, we then looked for galaxies lying within 20′ to 60′ of PSPC pointings and found 14 cases, four of which were either obscured by the PSPC support structure or too close to the edge of the field to be measurable. Of the other 10, nine were nondetections and one (NGC 3065) was detected. The counts for these sources were corrected for vignetting and are given in Table 1 as well.

In addition, we included those sample galaxies that were observed as part of the *ROSAT* All-Sky Survey (Beuing et al. 1999) but were not among the pointed observations. This provided a measure of the X-ray content for an additional 12 galaxies from the SS92 sample, although all but one of these (NGC 5982) were upper limits. The galaxies NGC 3377 and NGC 3379, which have *ROSAT* HRI (but no PSPC) observations, are also listed (from Brown & Bregman 1998) in Table 2.

Table 2 presents data for all sample galaxies with available H I mapping and/or *ROSAT* X-ray observations. The fine-structure Σ was taken from SS92. The total apparent blue magnitudes (B_T) were taken from the RC3 (de Vaucouleurs et al. 1991), and the distances (D) were taken from the Nearby Galaxies Catalog by Tully (1988) for galaxies within about 40 Mpc and from optical velocities given in the RC3 for more distant galaxies (assuming $H_0 = 75$ km s^{-1} Mpc^{-1}). Galaxies not detected in H I are listed as n/d in Table 2. Also listed in Table 2 is the logarithm of the ratio of the X-ray to blue luminosities, the "X-ray excess" $\log(L_X/L_B)$, with L_X in ergs per second and L_B in solar units ($L_{B_\odot}$).

Several sources appeared in both our list of *ROSAT* PSPC pointed observations and in the *ROSAT* survey data published by Beuing et al. (1999). As a way of checking the reliability of our measurements from the pointed data, we compared our count rates with those of Beuing et al. The results are plotted in Figure 1. We found that the count rates generally agreed to within a factor of 2. Where sources were undetected, the pointed data provided more stringent upper limits. There were a few detections where the rates differed by just over a factor of 2. These were NGC 7626, which has an asymmetric distribution of X-rays and is in the Pegasus I Cluster with other X-ray–emitting galaxies nearby; NGC 3226, which is very close to the X-ray–bright galaxy NGC 3227; and NGC 4203, which lies only 2′ from an apparently unrelated X-ray source of similar brightness. In NGC 3226 and NGC 4203, the extraneous sources lay well within the survey apertures used by Beuing et al. We have attempted to eliminate their counts from our analysis of the pointed data either by using smaller apertures (where

TABLE 1

ROSAT PSPC Data from Pointed Observations

System	Source Counts	Error Counts	R (arcmin)	Exposure (s)	$N_{\rm H\,I}$ (10^{20} cm^{-2})	Flux (ergs cm^{-2} s^{-1})	Error (ergs cm^{-2} s^{-1})
$R < 20'$:							
NGC 524	268.3	18.8	2	11171	4.53	0.300E−12	0.601E−13
NGC 596	<23.6	10.3	2	4055	2.46	<0.646E−13	0.292E−13
NGC 1052.....	474.9	27.7	2	13975	3.11	0.400E−12	0.743E−13
NGC 2300.....	1729.1	55.2	5	17446	6.39	0.142E−11	0.289E−12
NGC 2768.....	177.9	20.3	4	4766	4.24	0.466E−12	0.102E−12
NGC 3193.....	67.7	13.3	2	4617	3.39	0.172E−12	0.455E−13
NGC 3226.....	745.0	38.2	3	19547	3.54	0.448E−12	0.824E−13
NGC 3605.....	116.7	15.8	1	23853	2.88	0.576E−13	0.128E−13
NGC 3607.....	1637.9	68.3	4	23853	2.89	0.808E−12	0.146E−12
NGC 3608.....	500.1	32.0	2	23853	2.89	0.247E−12	0.463E−13
NGC 3610.....	146.6	20.6	2	10784	0.83	0.129E−12	0.203E−13
NGC 3640.....	125.9	19.4	2	15107	3.23	0.980E−13	0.230E−13
NGC 3998.....	38927.1	205.9	3	60722	1.32	0.622E−11	0.605E−12
NGC 4125.....	406.5	31.1	3	5707	1.45	0.692E−12	0.855E−13
NGC 4203.....	5345.7	74.4	1.5	22663	1.68	0.248E−11	0.264E−12
NGC 4261.....	2710.9	85.1	4	21893	1.99	0.133E−11	0.149E−12
NGC 4278.....	173.3	16.5	2	3411	1.88	0.535E−12	0.760E−13
NGC 4283.....	<19.9	8.7	2	3411	1.88	<0.627E−13	0.281E−13
NGC 4374.....	4054.3	73.4	2	33659	1.75	0.126E−11	0.953E−13
NGC 4382.....	411.2	50.2	4	8495	2.37	0.538E−12	0.888E−13
NGC 4552.....	1842.7	49.8	2	16660	1.68	0.116E−11	0.127E−12
NGC 4697.....	3359.1	128.0	5	45235	2.73	0.825E−12	0.969E−13
NGC 5273.....	152.8	16.8	2	5386	1.12	0.275E−12	0.403E−13
NGC 5322.....	700.5	46.2	2	34778	1.73	0.212E−12	0.263E−13
NGC 5846.....	3803.7	76.0	5	8804	3.96	0.540E−11	0.102E−11
NGC 7252.....	133.2	23.2	2	17371	2.28	0.852E−13	0.176E−13
NGC 7619.....	3548.5	97.3	7	18221	5.35	0.243E−11	0.461E−12
NGC 7626.....	515.1	29.4	2	18221	5.35	0.353E−12	0.693E−13
$20' < R < 60'$:							
NGC 584	<43.0	18.7	3	4055	2.49	<0.118E−12	0.528E−13
NGC 3032.....	<90.4	47.0	3	12206	2.73	<0.823E−13	0.437E−13
NGC 3065.....	339.6	41.2	3	10145	2.52	0.372E−12	0.612E−13
NGC 3921.....	<49.1	21.3	3	3851	1.17	<0.124E−12	0.551E−13
NGC 4168.....	<84.7	36.5	3	14300	2.01	<0.637E−13	0.283E−13
NGC 4660.....	<54.5	23.2	3	4138	2.12	<0.146E−12	0.644E−13
NGC 4915.....	<63.7	23.0	3	7429	2.87	<0.101E−12	0.405E−13
NGC 5198.....	<123.2	53.0	3	23956	1.73	<0.541E−13	0.240E−13
NGC 5557.....	<92.2	39.7	3	14242	1.09	<0.629E−13	0.277E−13
NGC 5831.....	<60.0	26.1	3	5941	4.37	<0.126E−12	0.598E−13

this appeared to include all the galaxy counts) or by subtracting the extraneous source counts from the counts in our galaxy apertures. Survey data were generally obtained with much shorter exposure times than pointed data. The larger point-spread functions for the survey data and for the pointed data beyond the central 20′ radius of the PSPC also exacerbated the problem of weak source detection. This is why many more galaxies were detected within the central regions of the pointed data (see Table 1). The pointed data clearly showed that the larger radii used by Beuing et al. included sources separate from the target galaxy. Figure 2 shows two examples. This effect contributes to the scatter in Figure 1 and also to the systematically lower rates measured from the pointed data. These rates are less affected by source confusion.

Our computed values of log (L_X/L_B) agree with published results within the errors for NGC 3610 and NGC 4125, both also measured from *ROSAT* pointed observations by Fabbiano & Schweizer (1995).

4. GAS PHASE VERSUS FINE STRUCTURE

Table 2 shows the compilation of optical, radio, and X-ray data for the sample galaxies for which these data were available. In this table, we list all the galaxies from SS92 with either H I mapping observations or *ROSAT* observations or both, arranged in order of decreasing Σ. This allows us to investigate how the cold and hot gas contents of E and S0 galaxies vary with fine structure.

For the cold gas content, we used our own data (Hibbard & Sansom 2000) and results from a program to map the H I in a sample of peculiar elliptical galaxies, kindly communicated by J. van Gorkom & D. Schiminovich (see, e.g., Schiminovich et al. 1994, 1995, 1997; van Gorkom & Schiminovich 1997). We also correlated the SS92 sample against the compilation of H I mapping observations by Martin (1998). Detection limits were calculated by taking the quoted 3 σ noise limits and adopting a velocity width of $\Delta v = 42$ km s^{-1}. While total H I line widths may be much wider than this, it is our experience that individual tidal

TABLE 2

GALAXIES FROM SS92 WITH H I MAPPING AND/OR *ROSAT* X-RAY OBSERVATIONS

System	Σ	B (mag)	D (Mpc)	$\log(M_{\rm H\,I})$ ($M_\odot$)	H I Morphology	H I Reference	$\log(L_X/L_B)$ (ergs $s^{-1} L_{B\odot}^{-1}$)
NGC 7252	10.1	12.06	63.5	9.72	Tidal tails	1	29.64
NGC 3921	8.84	13.06	77.9	9.56	Tidal tails	2	<30.20
NGC 3610	7.60	11.70	29.2	<6.90	n/d	3	29.68
NGC 3640	6.85	11.36	24.2	<6.85	n/d	3	29.42
NGC 4382 V.....	6.85	10.00	16.8	<6.60	n/d	3	29.62
NGC 7585	6.70	12.33	46.0	<7.64	n/d	4	...
NGC 4125	6.00	10.65	24.2	7.43	Outside body	5	29.99
NGC 7600	5.78	12.91	45.8	<7.64	n/d	4	...
NGC 4915	5.48	12.95	42.0	...	...	...	<30.07
NGC 0474	5.26	12.37	32.5	8.90	Tidal debris	6	...
NGC 5018	5.15	11.69	40.9	9.15	Bridge	7	<29.80[a]
NGC 0596	4.60	11.84	23.8	<7.08	n/d	4	<29.43
NGC 2911	4.48	12.50	41.8	9.25	Unknown	8	...
NGC 7332	4.00	12.02	18.2	<7.76	n/d	9	...
NGC 3226	3.70	12.30	23.4	~8.0	Near tidal tails	10	30.46
NGC 5831	3.60	12.45	28.5	...	...	...	<29.97
NGC 3065	3.48	13.50	31.3	...	...	...	30.86
NGC 4168 V.....	3.00	12.11	16.8	...	...	...	<29.53
NGC 2300	2.85	12.07	31.0	<7.30	n/d	4	30.87
NGC 0584	2.78	11.44	23.4	...	...	...	<29.53
NGC 5557	2.78	11.92	42.6	...	...	...	<29.45
NGC 3032	2.70	13.18	24.5	...	...	...	<30.07
NGC 3605	2.70	13.13	16.8	<7.46	n/d	9	29.90
NGC 7626	2.60	12.16	45.6	7.36	Outside body	3	30.30
NGC 2685	2.48	12.12	16.2	9.30	Polar ring	11	...
NGC 4374 V.....	2.30	10.09	16.8	<7.0	n/d	4	30.02
NGC 5576	2.30	11.85	26.4	<7.93	n/d	9	<29.82[a]
NGC 5982	2.04	12.04	38.7	...	...	...	30.48[a]
NGC 4552 V.....	2.00	10.73	16.8	<6.76	n/d	4	30.24
NGC 5322	2.00	11.14	31.6	<7.00	n/d	3	29.67
NGC 5198	1.85	12.69	39.0	...	...	...	<29.70
NGC 1052	1.78	11.41	17.8	8.69	Tidal tails	12	30.05
NGC 3156	1.70	13.07	18.6	...	...	...	<29.85[a]
NGC 0636	1.48	12.41	24.2	<7.08	n/d	4	<30.00[a]
NGC 3377	1.48	11.24	8.1	...	...	...	29.21[b]
NGC 4278	1.48	11.09	9.7	8.56	Disk	13	30.05
NGC 3818	1.30	12.67	25.1	...	...	...	<30.17[a]
NGC 3245	1.00	11.70	22.2	<7.38	n/d	8	...
NGC 4261	1.00	11.41	35.1	...	...	...	30.57
NGC 0524	0.70	11.30	32.1	...	...	...	29.88
NGC 5273	0.60	12.44	21.3	...	...	...	30.30
NGC 5846	0.30	11.05	28.5	...	...	...	31.04
NGC 2768	0.00	10.84	23.7	8.26	Outside body	14	29.89
NGC 2974	0.00	11.87	28.5	9.08	Disk	7	<29.67[a]
NGC 3193	0.00	11.83	23.2	<6.81	n/d	15	29.85
NGC 3379	0.00	10.24	8.1	9.04	200 kpc ring	16	29.29[b]
NGC 3607	0.00	10.82	19.9	<7.61	n/d	9	30.12
NGC 3608	0.00	11.70	23.4	<7.76	n/d	9	29.96
NGC 3998	0.00	11.61	21.6	8.85	Polar ring	17	31.32
NGC 4036	0.00	11.57	24.6	...	...	...	<29.60[a]
NGC 4203	0.00	11.80	9.7	8.85	Ring	18	31.00
NGC 4283	0.00	13.00	9.7	...	...	...	<29.88
NGC 4589	0.00	11.69	30.0	...	...	...	<29.49[a]
NGC 4660 V.....	0.00	12.16	16.8	...	...	...	<29.91
NGC 4697	0.00	10.14	23.3	...	...	...	29.86
NGC 5485	0.00	12.31	32.8	...	...	...	<29.72[a]
NGC 5574	0.00	13.23	28.7	<7.93	n/d	9	<30.39[a]
NGC 7457	0.00	12.09	12.3	<6.94	n/d	8	<29.77[a]
NGC 7619	0.00	12.10	50.7	7.48	Outside body	14	31.11

[a] Ratio from Beuing et al. (1999), using *ROSAT* survey data.

[b] Ratio from Brown & Bregman (1998), using *ROSAT* HRI data.

REFERENCES.—(1) Hibbard et al. 1994; (2) Hibbard & van Gorkom 1996; (3) Hibbard & Sansom 2000; (4) Schiminovich, van Gorkom, & van der Hulst 2000; (5) Rupen, private communication; (6) Schiminovich et al. 1997; (7) Kim et al. 1988; (8) Chamaraux, Balkowski, & Fontanelli 1987; (9) Haynes 1981; (10) Mundel et al. 1995; (11) Shane 1980; (12) van Gorkom et al. 1986; (13) Raimond et al. 1981; (14) Dijkstra et al. 2000; (15) Williams, McMahon, & van Gorkom 1991; (16) Schneider 1989; (17) Knapp, van Driel, & van Woerden 1985b; (18) van Driel & van Woerden 1991.

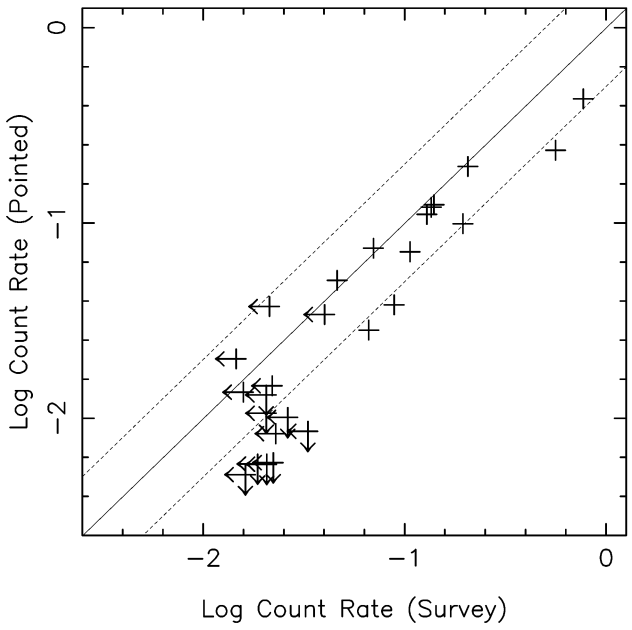

FIG. 1.—Comparison of count rates (counts s^{-1}) measured from the *ROSAT* survey data by Beuing et al. (1999) with the count rates measured from archival *ROSAT* PSPC pointed observations. The solid line represents the one-to-one correlation and the dashed lines are a factor of 2 on either side of this. The slightly lower average rates measured from the pointed data are less affected by source confusion and are, therefore, better estimates of the galaxy emission. Arrows indicate 3 σ upper limits to count rates for undetected sources.

features have relatively narrow line widths and that this smaller limit is appropriate for the detection of tidal H I. We define an "H I excess" as $\log(M_{\rm H\,I}/L_B)$, with the H I mass $M_{\rm H\,I}$ in solar masses and L_B in solar luminosities. This allows us to compare the cold and hot gas contents in a similar way.

Figure 3 shows the X-ray excess plotted against the fine-structure index for the *ROSAT* PSPC pointed data. Circles indicate H I detections. From this figure we find a trend for the X-ray excess to anticorrelate with fine structure. Including only X-ray detections, the Pearson correlation coefficient is $r = -0.47$, indicating a clear anticorrelation. The X-ray excess is large only in early-type galaxies with low levels of fine structure. Conversely, all galaxies with a high fine-structure index are X-ray weak.

To investigate this anticorrelation further we looked at how the vertical scatter in the L_X-L_B relation varies with fine structure. From *ROSAT* survey data, the mean L_X-L_B relation found for early-type galaxies by Beuing et al. (1999, especially Fig. 8) was

$$\log [L_X/(1 \text{ erg s}^{-1})] = 2.23 \log (L_B/L_{B_\odot}) + 17.02$$

(i.e., $L_X \propto L_B^{2.23}$). We used this relation to compute residuals, $\Delta \log L_X$, against the mean value of $\log L_X$ at any given $\log L_B$ and plotted these residuals versus the fine-structure Σ. Figure 4 shows the result. There is again an anticorrelation, similar in strength ($r = -0.44$) to the anticorrelation of X-ray excess with Σ. Early-type galaxies with a high fine-structure index all lie *below* the mean L_X-L_B relation, indicating that they are deficient in hot gas.

Galaxies with detected H I are shown as circled plus signs in Figures 3 and 4. From these figures, we see no trend of H I detection probability with X-ray excess or with Σ. H I detections appear in all types of galaxies plotted. The two merger remnants have H I detected in tidal tails (see Table 2). The galaxy with the highest Σ is the $\sim$0.5–0.7 Gyr old merger remnant NGC 7252, which has 5×10^9 $M_\odot$ of H I in its tidal tails, yet a dearth of H I at its center (Hibbard et al. 1994). Table 2 shows that there are a few other E and S0 galaxies with high fine-structure content ($3 < \Sigma < 8$) that feature H I in tidal tails or outside the galaxy. From Table 2, all instances of H I in rings or disks occur in galaxies of lower Σ. These galaxies cover a range of X-ray excesses. Therefore, we see a weak trend of H I morphology (but not of detection probability) with fine structure.

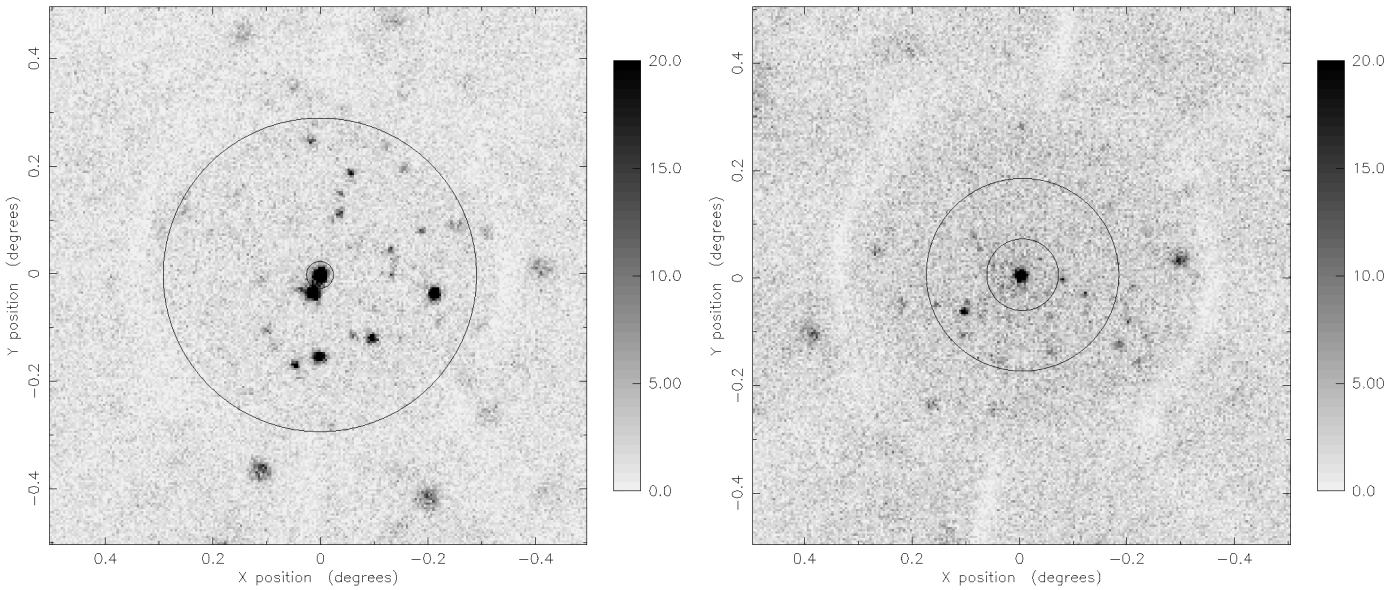

FIG. 2.—Examples of two *ROSAT* pointed images showing a 1° square field around the PSPC field center in each case. The galaxies being measured are NGC 4203 in the left image and NGC 4261 in the right image. These images illustrate the source confusion affecting the data included in the apertures used on survey data by Beuing et al. 1999 (*large circles*). The pointed data reduce this confusion without missing galaxy light (*smaller circles*). The keys are in counts per pixel.

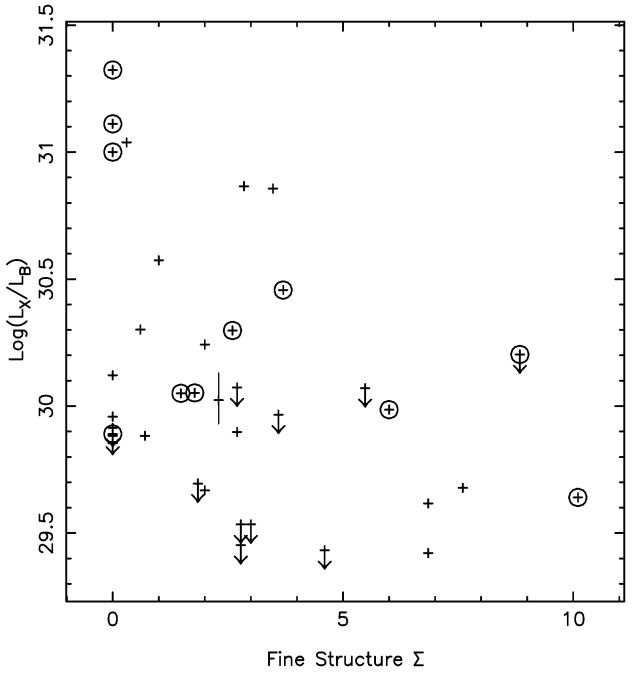

FIG. 3.—X-ray excess log (L_X/L_B) (in ergs s^{-1} $L_{B_\odot}^{-1}$) plotted vs. optical fine-structure index Σ for 38 galaxies from the SS92 sample. The plotted data are from *ROSAT* PSPC pointed observations. Plus signs indicate X-ray detections, while the arrows indicate 3 σ upper limits. Circled plus signs have associated H I detections. The vertical bar indicates typical errors.

In Figure 5, we plot both the X-ray excess and the measured H I excess versus the fine-structure index. Data from all the galaxies listed in Table 2 are included in this plot, with data points coded by galaxy type. Data points representing elliptical and S0 galaxies from the sample of SS92 are drawn as filled and open squares, respectively.

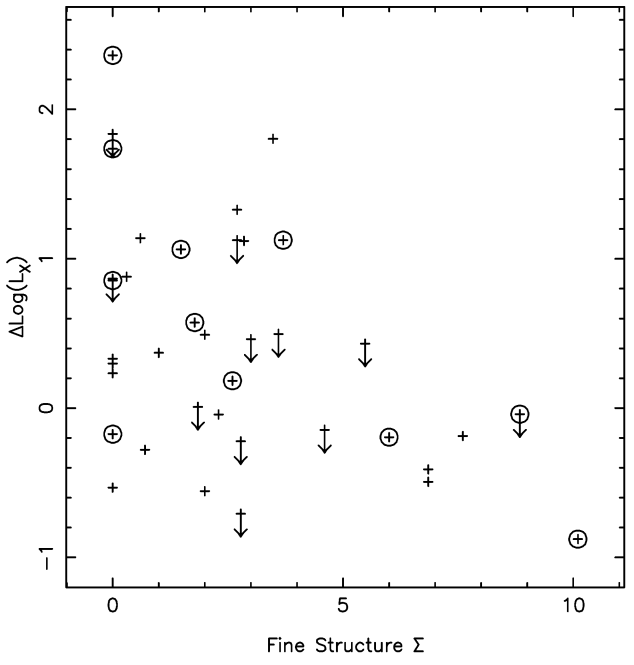

FIG. 4.—Residuals, Δ log L_X (in ergs s^{-1}), against the mean L_X-L_B relation plotted vs. the fine-structure index Σ. The symbols are as in Fig. 3. The X-ray data plotted are only those obtained from *ROSAT* PSPC pointed observations.

The merger remnants, NGC 7252 and NGC 3921, are represented by filled circles. Galaxies with active galactic nuclei (AGNs; from Véron-Cetty & Véron 1996) are plotted as plus signs. Apart from the Seyfert galaxy NGC 3998, which has the highest X-ray excess of our sample, the other four galaxies with AGNs (NGC 2768, 3032, 4278, and 5273) and three LINERs (NGC 1052, 3226, and 4036) are not extreme cases. Therefore, the effect of X-ray emission from active nuclei appears to be relatively small in these plots.

The top plot shows no clear trend of atomic gas with increasing Σ. In fact, the elliptical and S0 galaxies with the highest Σ lie much lower in this plot than the two merger remnants, indicating a dearth of H I. This is contrary to the naive expectation that recent merger remnants might have copious amounts of tidally ejected H I present in their outer regions, gas that then gradually falls back into the remnant's body (Hibbard & Mihos 1995). We address this issue in more detail in Hibbard & Sansom (2000), where we discuss the possibilities that some high-Σ systems may not be recent (less than a few gigayears old) merger remnants of *gas-rich* galaxies; H I tidal tails may not survive for more than a few gigayears, or the survivability of tidal H I may depend on other factors.

In the two bottom panels of Figure 5, we plot log (L_X/L_B) against both Σ and log($M_{H\,I}/L_B$). The plot of X-ray excess against neutral gas excess shows no discernible trend—there are X-ray–luminous galaxies both with large amounts of H I and with stringent limits on H I. This shows that there exists no clear relationship between the cold and hot gas phases for this sample of galaxies. The lack of H I and the low X-ray excess measured in relaxed, early-type galaxies with high Σ (see Table 2) imply a distinct lack of cold *and* hot gas in these suspected late merger remnants. Yet, gas is expected to have fallen back in from the tidal tails. If these galaxies are the ancient remnants of disk-disk mergers, then it is not clear where the cold gas formerly associated with the progenitors is now. It may have been ionized by the star formation associated with the merger, efficiently formed into stars, cooled to molecular form, or lost from the system. In major mergers, a fair amount of the gas is known to turn into stars, partially via the central-disk phenomenon (Schweizer 1998, especially § 5.3). In future work, we will investigate the molecular gas content of this sample to check if they have unusually large quantities of molecular gas when compared with early-type galaxies as a class (Roberts et al. 1991).

We also looked for environmental effects on the X-ray excess of the sample galaxies. We found no correlations between the X-ray excess and Tully's (1988) local galaxy density parameter, ρ. Most of the galaxies in this sample are field objects or members of small groups. Five galaxies are Virgo Cluster members (marked by a "V" in Table 2). These five galaxies cover a range of Σ and X-ray excess. They are not all X-ray luminous. Therefore, we find no evidence for any environmental effect on the X-ray excess or its anticorrelation with Σ in this sample.

Figure 5 shows that there are no clear trends between the hot and cold gas contents of these galaxies. However, there is a clear anticorrelation between the X-ray excess and the amount of fine structure. As the bottom left panel of Figure 5 shows, there is a remarkable lack of galaxies with high Σ and large X-ray excess. We find that the *ROSAT* survey data of Beuing et al. also display this trend. This anticorrelation was discovered for two high fine-structure gal-

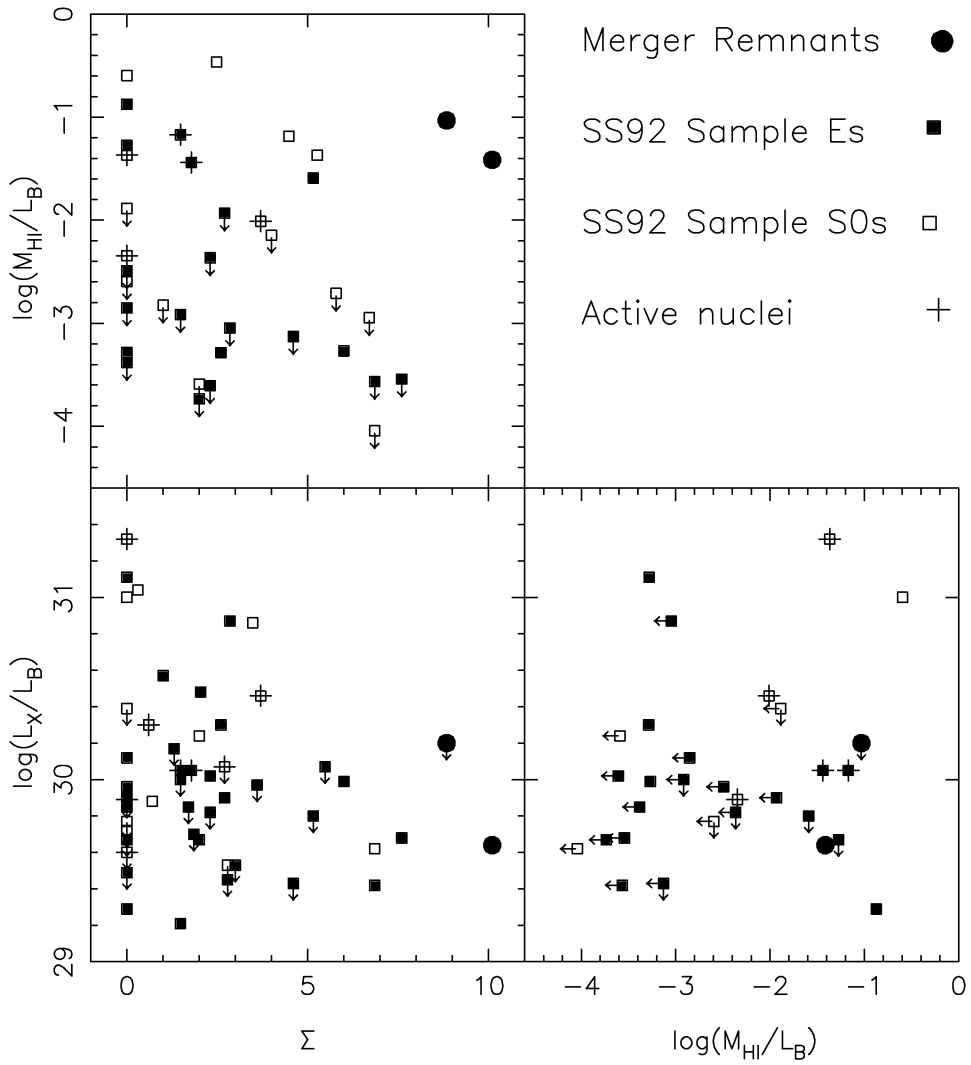

FIG. 5.—Composite plot showing cold and hot gas content vs. Σ. Elliptical galaxies are shown as filled squares, S0 galaxies as open squares, and the two recent merger remnants NGC 7252 and NGC 3921 as circles. Attached arrows indicate 3 σ upper limits. The three panels show the parameters of cold gas excess [$\log(M_{\rm H\,I}/L_B)$ in $M_\odot\ L_{B_\odot}^{-1}$], hot gas excess [$\log(L_X/L_B)$ in ergs $s^{-1}\ L_{B_\odot}^{-1}$], and fine-structure index (Σ) plotted against each other. The X-ray data plotted include all SS92 galaxies observed with *ROSAT*, as listed in Table 2. Note the apparent anticorrelation between $\log(L_X/L_B)$ and Σ.

axies by Fabbiano & Schweizer (1995), and further quantified by Mackie & Fabbiano (1997), and is discussed by Schweizer (1998, especially p. 198). Peculiar E and S0 galaxies with high fine-structure content tend to be X-ray weak, consistent with X-ray emission from stellar sources alone. For example, $\log(L_X/L_B)$ is 29.54 (in the 0.5–2 keV band) for the bulge of M31, with nearly equal contributions from the hard and soft emission from low-mass X-ray binaries (Irwin & Sarazin 1998). The anticorrelation between fine structure and X-ray excess found in this work supports the suggestion made by Fabbiano & Schweizer (1995) that merger remnants are X-ray weak. These authors suggest that a merger-induced starburst drives a galactic superwind, which clears the remnant of most hot gas. After the starburst subsides, the hot gas is gradually replenished by stellar mass loss (Sandage 1957; Faber & Gallagher 1976; Forman, Jones, & Tucker 1985; Sarazin 1997) and, perhaps to some small extent, also by the thermalization of returning tidal debris (Hibbard & van Gorkom 1996), although the $\log(L_X/L_B)$ versus $\log(M_{\rm H\,I}/L_B)$ plot argues against the latter being the primary source of X-ray halos.

This suggests either that the timescale for creating hot halos in early-type galaxies is long (a few gigayears), regardless of the cold gas content of the progenitors, or that E/S0 galaxies made in different ways have different X-ray properties, with merger remnants forming a distinguishable, X-ray–underluminous class. The range of $\log(L_X/L_B)$ values in Figure 3 suggests that the long timescale for halo production is more likely: we do not see a dichotomy of behavior but, rather, a gradual change of X-ray excess with Σ.

5. SUMMARY

We have searched for correlations between the cold gas content, hot gas content, and fine-structure index Σ of early-type galaxies. We find no correlation of H I content or H I detection probability with Σ. In particular, we do not observe any tendency for high-Σ systems to have large amounts of tidal H I. Also, the H I content does not correlate with the hot gas content as measured by the X-ray excess.

However, we do observe an anticorrelation between Σ and X-ray excess. We find that E and S0 galaxies with high

fine-structure content—thought to be remnants of ancient mergers ("King gap galaxies")—have low X-ray luminosities. This indicates that these galaxies, when compared with early-type galaxies with little or no fine structure, are deficient in hot gas. During mergers, X-ray emission from hot gas is seen to rise (with evidence for outflows) and then fall after a relatively short time (Read & Ponman 1998). This and the current results are consistent with hot halos forming in early-type galaxies over a timescale of several gigayears. Hence, such halos tend to appear *after* the morphological disturbances from past mergers have faded away. If one excludes galaxies with AGNs, only normal E and S0 galaxies with *low* levels of fine structure (i.e., relaxed systems) are strong X-ray emitters, with emission well in excess of the contribution expected from stars.

We thank Jacqueline van Gorkom and David Schiminovich for permission to refer to their results ahead of publication, and Keith Arnaud for the use of his code for hydrogen column densities. This research has made use of data obtained from the Leicester Database and Archive Service at the department of Physics and Astronomy, Leicester University, UK. F. S. gratefully acknowledges partial support from NSF through grants AST 95-29263 and AST 99-00742.

REFERENCES

Barnes, J. E. 1994, in The Formation and Evolution of Galaxies, ed. C. Muñoz-Tuñón & G. Sánchez (Cambridge: Cambridge Univ. Press), 399
Bender, R., & Surma, P. 1992, A&A, 258, 250
Beuing, J., Döbereiner, S., Böhringer, H., & Bender, R. 1999, MNRAS, 302, 209
Bregman, J. N., Hogg, D. E., & Roberts, M. S. 1992, ApJ, 387, 484
Brown, B. A., & Bregman, J. N. 1998, ApJ, 495, L75
Chamaraux, P., Balkowski, C., & Fontanelli, P. 1987, A&AS, 69, 263
de Vaucouleurs, G., de Vaucouleurs, A., Corwin, H. G., Jr., Buta, R. J., Paturel, G., & Fouqué, P. 1991, Third Reference Catalogue of Bright Galaxies (New York: Springer) (RC3)
Dijkstra, R., van Gorkom, J. H., van der Hulst, T., & Schminovich, D. 2000, in preparation
Fabbiano, G., Kim, D.-W., & Trinchieri, G. 1992, ApJS, 80, 531
Fabbiano, G., & Schweizer, F. 1995, ApJ, 447, 572
Faber, S. M., & Gallagher, J. S. 1976, ApJ, 204, 365
Forman, W., Jones, C., & Tucker, W. 1985, ApJ, 293, 102
Haynes, M. P. 1981, AJ, 86, 1126
Hibbard, J. E., Guhathakurta, P., van Gorkom, J. H., & Schweizer, F. 1994, AJ, 107, 67
Hibbard, J. E., & Mihos, J. C. 1995, AJ, 110, 140
Hibbard, J. E., & Sansom, A. E. 2000, in preparation
Hibbard, J. E., & van Gorkom, J. H. 1996, AJ, 111, 655
Irwin, J. A., & Sarazin, C. L. 1998, ApJ, 499, 650
Kim, D.-W., Guhathakurta, P., van Gorkom, J. H., Jura, M., & Knapp, G. R. 1988, ApJ, 330, 684
Knapp, G. R., Turner, E. L., & Cunniffe, P. E. 1985a, AJ, 90, 454
Knapp, G. R., van Driel, W., & van Woerden, H. 1985b, A&A, 142, 1
Lees, J. F., Knapp, G. R., Rupen, M. P., & Phillips, T. G. 1991, ApJ, 379, 177
Mackie, G., & Fabbiano, G. 1997, in ASP Conf. Ser. 116, The Nature of Elliptical Galaxies, ed. M. Arnaboldi, G. S. Da Costa, & P. Saha (San Francisco: ASP), 401
Martin, M. C. 1998, A&AS, 131, 73
Mundell, C. G., Pedlar, A., Axon, D. J., Meaburn, J., & Unger, S. W. 1995, MNRAS, 277, 641
Raimond, E., Faber, S. M., Gallagher, J. S., & Knapp, G. R. 1981, ApJ, 246, 708
Read, A. M., & Ponman, T. J. 1998, MNRAS, 297, 143
Roberts, M. S., Hogg, D. E., Bregman, J. N., Forman, W. R., & Jones, C. 1991, ApJS, 75, 751
Sandage, A. 1957, ApJ, 125, 422
Sarazin, C. L. 1997, in ASP Conf. Ser. 116, The Nature of Elliptical Galaxies, ed. M. Arnaboldi, G. S. Da Costa, & P. Saha (San Francisco: ASP), 375
Schiminovich, D., van Gorkom, J. H., & van der Hulst, T. 2000, in preparation
Schiminovich, D., van Gorkom, J. H., van der Hulst, J. M., & Kasaw, S. 1994, ApJ, 423, L101
Schiminovich, D., van Gorkom, J. H., van der Hulst, J. M., & Malin, D. F. 1995, ApJ, 444, L77
Schiminovich, D., van Gorkom, J., van der Hulst, T., Oosterloo, T., & Wilkinson, A. 1997, in ASP Conf. Ser. 116, The Nature of Elliptical Galaxies, ed. M. Arnaboldi, G. S. Da Costa, & P. Saha (San Francisco: ASP), 362
Schneider, S. E. 1989, ApJ, 343, 94
Schweizer, F. 1986, Science, 231, 227
———. 1996, AJ, 111, 109
———. 1998, in Galaxies: Interactions and Induced Star Formation, ed. D. Friedli, L. Martinet, & D. Pfenniger (New York: Springer), 105
Schweizer, F., & Seitzer, P. 1992, AJ, 104, 1039 (SS92)
Schweizer, F., Seitzer, P., Faber, S. M., Burstein, D., Dalle Ore, C. M., & Gonzalez, J. J. 1990, ApJ, 364, L33
Shane, W. W. 1980, A&A, 82, 314
Stark, A. A., Gammie, C. F., Wilson, R. W., Bally, J., Linke, R., Heiles, C., & Hurwitz, M. 1992, ApJS, 79, 77
Toomre, A. 1977, in The Evolution of Galaxies and Stellar Populations, ed. B. M. Tinsley & R. B. Larson (New Haven: Yale Univ. Press), 401
Toomre, A., & Toomre, J. 1972, ApJ, 178, 623
Tully, R. B. 1988, Nearby Galaxies Catalog (Cambridge: Cambridge Univ. Press)
van Driel, W., & van Woerden, H. 1991, A&A, 243, 71
van Gorkom, J. H., Knapp, G. R., Raimond, E., Faber, S. M., & Gallagher, J. S. 1986, AJ, 91, 791
van Gorkom, J., & Schiminovich, D. 1997, in ASP Conf. Ser. 116, The Nature of Elliptical Galaxies, ed. M. Arnaboldi, G. S. Da Costa, & P. Saha (San Francisco: ASP), 310
Véron-Cetty, M.-P., & Véron, P. 1996, A Catalogue of Quasars and Active Nuclei (ESO Sci. Rep. 17) (Garching: ESO)
Williams, B. A., McMahon, R. M., & van Gorkom, J. H. 1991, AJ, 101, 1957